Antideuteron yield at the AGS and coalescence implications

T. A. Armstrong,(8,*) K. N. Barish,(3) S. Batsouli,(13) S. J. Bennett,(12) M. Bertaina,(7,†) A. Chikanian,(13) S. D. Coe,(13,‡) T. M. Cormier,(12) R. Davies,(9,§) C. B. Dover,(1,‖) P. Fachini,(12) B. Fadem,(5) L. E. Finch,(13) N. K. George,(13) S. V. Greene,(11) P. Haridas,(7,¶) J. C. Hill,(5) A. S. Hirsch,(9) R. Hoversten,(5) H. Z. Huang,(2) H. Jaradat,(12) B. S. Kumar,(13,**) T. Lainis,(10) J. G. Lajoie,(5) Q. Li,(12) B. Libby,(5,††) R. D. Majka,(13) T. E. Miller,(11) M. G. Munhoz,(12) J. L. Nagle,(4) I. A. Pless,(7) J. K. Pope,(13,‡‡) N. T. Porile,(9) C. A. Pruneau,(12) M. S. Z. Rabin,(6) J. D. Reid,(11) A. Rimai,(9,§§) A. Rose,(11) F. S. Rotondo,(13,‖‖) J. Sandweiss,(13) R. P. Scharenberg,(9) A. J. Slaughter,(13) G. A. Smith,(8) M. L. Tincknell,(9,¶¶) W. S. Toothacker,(8) G. Van Buren,(7,2) F. K. Wohn,(5) Z. Xu(13)

(E864 Collaboration)

(1) *Brookhaven National Laboratory, Upton, New York 11973*
(2) *University of California at Los Angeles, Los Angeles, California 90095*
(3) *University of California at Riverside, Riverside, California 92521*
(4) *Columbia University, Nevis Laboratory, Irvington, New York 10533*
(5) *Iowa State University, Ames, Iowa 50011*
(6) *University of Massachusetts, Amherst, Massachusetts 01003*
(7) *Massachusetts Institute of Technology, Cambridge, Massachusetts 02139*
(8) *Pennsylvania State University, University Park, Pennsylvania 16802*
(9) *Purdue University, West Lafayette, Indiana 47907*
(10) *United States Military Academy, West Point 10096*
(11) *Vanderbilt University, Nashville, Tennessee 37235*
(12) *Wayne State University, Detroit, Michigan 48201*
(13) *Yale University, New Haven, Connecticut 06520*

(February 3, 2000)

We present the results of Experiment 864's measurement of antideuteron yields in 11.5 GeV/c per nucleon Au + Pt collisions at the AGS. The analysis includes 250 million triggers representing 14 billion 10% central interactions sampled for events with high mass candidates. Antideuteron invariant yields are found to be $(1/2\pi p_t)d^2N/dydp_t = 3.5 \pm 1.5(stat.)^{+0.9}_{-0.5}(sys.) \times 10^{-8}$ GeV$^{-2}c^2$ in the rapidity range between $y = 1.8$ and 2.2 ($y_{cm} = 1.6$) for $<p_t>= 0.35$ GeV/c and $3.7 \pm 2.7(stat.)^{+1.4}_{-1.5}(sys.) \times 10^{-8}$ GeV$^{-2}c^2$ between rapidities $y = 1.4$ and 1.8 at $<p_t>= 0.26$ GeV/c. These yields, along with E864 antiproton measurements, lead to a most probable value for the coalescence factor $\overline{B_2}$ of $4.1 \pm 2.9(stat.)^{+2.3}_{-2.4}(sys.) \times 10^{-3}$ GeV$^2c^{-3}$ after correcting antiproton yields for antihyperon feeddown contributions. Implications for the coalescence model and antimatter annihilation are also discussed.

PACS numbers: 25.75.Dw, 25.75.Gz

I. INTRODUCTION

The production of antinucleons and antinuclei in heavy ion collisions is of significant interest for several reasons [1–3]. Because the initial colliding system contains no antibaryons, their yields and spectra are determined solely by collision dynamics. At AGS energies ($\sqrt{s} =$ 4.8 A GeV), nucleon-antinucleon pair production is above threshold in individual $Nucleon + Nucleon$ collisions, but direct deuteron-antideuteron pair production is not. However, a small fraction of the colliding nucleon pairs which have high relative Fermi momenta may exceed the threshold for d-$\overline{d}$ pair production. We have estimated this contributes at a level at least two orders of magnitude below the measured yield from our experiment. Antideuterons are therefore predominantly formed in secondary interactions between directly produced antinucleons from the collision. Their production is then highly dependent on the total abundances and spatial distribution of the antinucleons.

Simple coalescence and thermal models [4–6] indicate that differences in the measurement of the coalescence parameter between nuclei (B_A) and their antinuclei counterparts ($\overline{B_A}$) are due to differences in the source volumes, where

$$B_A \equiv \frac{\left(\frac{1}{2\pi p_t}\frac{d^2N_A}{dydp_t}\right)}{\left(\frac{1}{2\pi p_t}\frac{d^2N_p}{dydp_t}\right)^Z \left(\frac{1}{2\pi p_t}\frac{d^2N_n}{dydp_t}\right)^{A-Z}} \quad (1)$$

$$\approx \frac{\left(\frac{1}{2\pi p_t}\frac{d^2N_A}{dydp_t}\right)}{\left(\frac{1}{2\pi p_t}\frac{d^2N_p}{dydp_t}\right)^A}, \quad (2)$$

$$\overline{B_A} \approx \frac{\left(\frac{1}{2\pi p_t}\frac{d^2N_{\overline{A}}}{dydp_t}\right)}{\left(\frac{1}{2\pi p_t}\frac{d^2N_{\overline{p}}}{dydp_t}\right)^A}. \quad (3)$$

We have used an assumption in Equation 2 that neutron and proton abundances in the region of the measurement are similar, which is only approximately true [7]. Antineutron yields remain unmeasured.

The small binding energy of (anti)deuterons requires that they be formed near the hypersurface of the fireball where their mean free path is sufficiently large that they suffer no further collisions. The additional annihilation cross section for antinucleons implies that densities must be even lower for antideuterons than deuterons to have sufficient mean free paths for survival [8], possibly resulting in a more shell-like spatial formation zone for antideuterons [9]. This has fueled predictions that $\overline{B_2}$ will be notably smaller than B_2 [8–10].

However, other thermal model calculations suggest B_2 and $\overline{B_2}$ may be very similar. Microscopic models demonstrate that nucleons may undergo 20-30 collisions before their final interactions in heavy ion collisions at AGS and SPS energies [11,12]. The more collisions the constituents undergo, the further towards thermal and chemical equilibrium the system is driven. If equilibrium is complete, and all particles freeze-out along the same hypersurface, no difference would be expected between B_2 and $\overline{B_2}$ [13]. An analysis of equilibrium conditions in the collisions studied by E864 is presented elsewhere [14].

A sample of two antideuterons was previously measured in the AGS Experiment 858 in minimum bias Si + Au collisions at 14.6 GeV/c per nucleon, indicating that in such a system $\overline{B_2}$ is below or at the level of B_2 [15]. However, this measurement involves a smaller system size where antimatter annihilation may not be as prominent as in central Au + Pt collisions. Antiproton yields are significantly suppressed from first collision scaling in the larger colliding systems compared to peripheral collisions or Si + Au collisions [16]. Some transport models [3] indicate that over 90% of the originally produced antiprotons are annihilated, while other calculations include a screening of the annihilation in this dense environment thus reducing the losses [17]. These large collisions, consequently, provide a good place to see the effects of annihilation on antideuteron production. Interestingly, there may be additional processes in these collisions whose contributions to antimatter coalescence rates are not completely understood, such as findings that a significant portion of the antibaryon number is carried away in the form of strange antibaryons [18].

II. EXPERIMENT

In order to search for rare products from heavy ion collisions at the AGS, Experiment 864 was designed as an open geometry, high rate spectrometer [19]. It features a multiplicity detector for triggering on central collisions [20], and a level 2 trigger capable of selecting events in which high mass objects traverse the spectrometer, using a hadronic calorimeter to provide fast energy and time measurements [21,22]. The calorimeter energy measurement encompasses the kinetic energy for normal hadronic matter, with an additional annihilation energy of approximately twice the particle mass for antimatter. Tracking of charged particles is performed primarily with three scintillating hodoscope TOF walls interspersed with two straw tube tracking stations for improved track spatial resolution. The tracking system is used to determine velocities and rigidities of charged particles accurately, providing mass resolutions typically better than 5% [19].

The spectrometer magnets can be set to different field strengths and polarities which optimize acceptance for particles of interest. During the 1996-1997 run of the experiment, over 250 million triggers were taken with both magnets set to -0.75T. This setting allows reasonable acceptance for antideuterons while most positively charged particles and lighter negatively charged particles are swept out of the acceptance. Figure 1 shows the antideuteron geometric acceptance for this field setting.

III. ANALYSIS

Figure 2a shows the mass spectrum of charge -1 particles from the data set in the region near the antideuteron mass ($1.8 < y < 2.2$) for tracks which have passed basic quality cuts. Simulations have been performed to study the background evident in the data, which is understood to have two predominant sources. In the rapidity range shown in Figure 2a, the background is dominated by neutrons passing through the spectrometer magnets before undergoing charge-exchange reactions ($n + X \to p + X'$), resulting in stiff tracks which are calculated with incorrect masses and charge signs. However, the energy measured by E864's hadronic calorimeter should be consistent with the kinetic energy of a proton traveling at the speed calculated from the hodoscope TOF measurements [22]. This energy measurement can then be used to cut away background whose calorimeter response is reasonably consistent with that of a proton. Such a cut is used in the mass spectrum shown in Figure 2b, revealing a clear peak at the antideuteron mass. The chosen cut requires that the calorimeter response is greater than 4σ above the expected response for a proton in order to remove as much background as possible without destroying the antideuteron signal (the cut is 95% efficient for antideuterons, aided by the significant energy contributions from annihilation in the calorimeter). While a 4σ cut would normally be expected to remove nearly 100% of the scattered protons, the efficiency is reduced in this case because of the bias from the level 2 trigger in selecting candidates whose calorimeter responses are large. Because this cut is independent of the background's calculated mass, the shape of the background is unaffected. A fit to the shape is made before the cut and used in fitting for signal plus background after the cut. The resulting antideuteron yield is 17.6 ± 7.5 counts, where the statistical error includes contributions from a background of $34.1 \pm 5.8(Poisson\ stat.) \pm 2.3(normalization)$.

Similarly, in the rapidity range between 1.4 and 1.8 the background is understood to be dominated by antiprotons which have scattered by small angles near the spectrometer magnets. Again, the calorimeter can be used to reject antiprotons in the mass spectrum, although the additional energy deposited from annihilation in the calorimeter leads to a smaller separation from antideuterons for antiprotons than protons. A 4σ cut would severely impinge upon the antideuteron signal, so a less stringent 2σ cut is chosen with the resulting efficiency for antideuterons at 86%. An antideuteron signal is found with 4.6 ± 3.3 counts, where the statistical error includes contributions from a background of $5.4 \pm 2.3(Poisson\ stat.) \pm 0.7(normalization)$.

In order to calculate invariant yields, the transverse momentum distribution of the measured antideuterons must also be understood as well as possible. Because it is not known which candidates under the mass peak are the true antideuterons, the p_t distribution is calculated for random selections of the candidates. For each selection, the acceptance-corrected count is determined by acceptance correcting every candidate at its measured y and p_t. Millions of random selections are made and a distribution of acceptance-corrected counts is found with a most probable value and widths which indicate the systematic errors of the method. Between the rapidities of 1.8 and 2.2, the candidates have an acceptance-weighted $<p_t>$ of 0.35 GeV/c, and have an upper limit of $p_t = 1$ GeV/c. Correcting for all efficiencies results in an antideuteron invariant yield of $3.5 \pm 1.5(stat.)^{+0.9}_{-0.5}(sys.) \times 10^{-8}$ GeV$^{-2}c^2$.

In the rapidity range between 1.4 and 1.8, the candidates have an acceptance-weighted $<p_t>$ of 0.26 GeV/c, and have an upper limit of $p_t = 0.5$ GeV/c. All possible selections of the candidates are tried, determining a yield of $3.7 \pm 2.7(stat.)^{+1.4}_{-1.5}(sys.) \times 10^{-8}$ GeV$^{-2}c^2$.

E864 has also measured antiproton yields in 10% central Au + Pb collisions at 11.5 GeV/c per nucleon [18]. These yields are shown along with the new antideuteron measurements in Figure 3 reflected about mid-rapidity. The new antideuteron yields are in agreement with upper limits previously published by E864 taken from a smaller data sample [18].

The measured antiproton and antideuteron yields allow us to calculate the coalescence factor $\overline{B_2}$ using Equation 3. The E864 antiproton measurement must be corrected for contributions from antihyperon decays as these do not participate in the coalescence process. Here, we will use the most probable value for $\overline{Y}/\overline{p} = 3.5$, and use the 98% confidence limit of $\overline{Y}/\overline{p} > 2.3$ to define the systematic error of the correction [18]. Additionally, as coalescence is a process affecting co-moving nucleons, yields must be taken at the same $<p_t>/A$. In the mid-rapidity bin ($1.4 < y < 1.8$), this means using the antiproton yield at $p_t = 0.13$ GeV/c, for which E864's antiproton measurements are valid. The final value of $\overline{B_2}$ comes out as $4.1 \pm 2.9(stat.)^{+2.3}_{-2.4}(sys.) \times 10^{-3}$ GeV$^2c^{-3}$, where the systematic error includes contributions from the antideuteron acceptance correction and the antihyperon-feeddown correction to the antiprotons.

E864 has also measured B_2 in the range $0.1 < p_t/A < 0.2$ GeV/c as $1.06 \pm 0.15 \times 10^{-3}$ GeV$^2c^{-3}$ [23]. While E864's $\overline{B_2}$ measurement is above its B_2 measurement, the two are within statistical and systematic errors of each other. These values are shown in Figure 4 along with those from other experiments studying collisions with very large numbers of participant nucleons ($\sim$400). Along with the SPS results, the evidence at this point suggests that there may be no difference between coalescence of matter and antimatter in central heavy ion collisions. This may be an indication that the freeze-out hypersurface for antideuterons is not substantially modified by antimatter annihilation from that of deuterons.

IV. SUMMARY AND ACKNOWLEDGEMENTS

E864 has measured an antideuteron signal in central heavy ion collisions at the AGS, where coalescence is likely to be the dominant method for production. The measured invariant yields are $3.5 \pm 1.5(stat.)^{+0.9}_{-0.5}(sys.) \times 10^{-8}$ GeV$^{-2}c^2$ ($1.8 < y < 2.2$, $<p_t>= 0.35$ GeV/c) and $3.7 \pm 2.7(stat.)^{+1.4}_{-1.5}(sys.) \times 10^{-8}$ GeV$^{-2}c^2$ ($1.4 < y < 1.8$, $<p_t>= 0.26$ GeV/c). The measured coalescence parameters from E864 for matter ($B_2 = 1.06 \pm 0.15 \times 10^{-3}$ GeV$^2c^{-3}$) and antimatter ($\overline{B_2} = 4.1 \pm 2.9(stat.)^{+2.3}_{-2.4}(sys.) \times 10^{-3}$ GeV$^2c^{-3}$) at mid-rapidity are within statistical and systematic errors of each other.

We gratefully acknowledge the excellent support of the AGS staff. This work was supported in part by grants from the U.S. Department of Energy's High Energy and Nuclear Physics Divisions, the U.S. National Science Foundation.

∗ Present address: Vanderbilt University, Nashville, Tennessee 37235

† Present address: Istituto di Cosmo-Geofisica del CNR, Torino, Italy / INFN Torino, Italy

‡ Present address: Anderson Consulting, Hartford, CT

§ Present address: Univ. of Denver, Denver CO 80208

‖ Deceased.

¶ Present address: Cambridge Systematics, Cambridge, MA 02139

∗∗ Present address: McKinsey & Co., New York, NY 10022

†† Present address: Department of Radiation Oncology, Medical College of Virginia, Richmond, VA 23298

‡‡ Present address: University of Tennessee, Knoxville, TN 37996

§§ Present address: Institut de Physique Nucléaire, 91406 Orsay Cedex, France

‖‖ Present address: Institute for Defense Analysis, Alexandria, VA 22311

¶¶ Present address: MIT Lincoln Laboratory, Lexington, MA 02420-9185

[1] S. Gavin *et al.*, Phys. Lett. B **234** (1990) 175
[2] V. Koch, G. E. Brown, and C. M. Ko, Phys. Lett. B **265** (1989) 29
[3] J. L. Nagle *et al.*, Phys. Rev. Lett. **73** (1994) 1219
[4] A. Schwarzchild and C. Zupancic, Phys. Rev. **129** (1963) 854
[5] R. Bond *et al.*, Phys. Lett. B **71** (1977) 43
[6] H. Sato *et al.*, Phys. Lett. B **98** (1981) 153
[7] T. A. Armstrong *et al.*, Phys. Rev. C **60** (1999) 064903
[8] S. Leupold and U. Heinz, Phys. Rev. C **50** (1994) 1110
[9] S. Mrowczynski, Phys. Lett. B **24** (1990) 459
[10] M. Bleicher *et al.*, Phys. Lett. B **361** (1995) 10
[11] L. V. Bravina *et al.*, Phys. Rev. C **60** (1999) 044905
[12] L. V. Bravina *et al.*, Phys. Lett. B **434** (1998) 379; L. V. Bravina *et al.*, Phys. Rev. C **60** (1999) 024904
[13] R. Scheibl and U. Heinz, Phys. Rev. C **59** (1999) 1585
[14] Z. Xu *et al.*, XXIX International Symposium on Multiparticle Dynamics (1999), nucl-ex/9909012
[15] M. Aoki *et al.*, Phys. Rev. Lett. **69** (1992) 2345
[16] D. Beavis *et al.*, Phys. Rev. Lett. **75** (1995) 3633; M. Bennett *et al.*, Phys. Rev. C **56** (1997) 1521
[17] S. H. Kahana, Y. Pang, T. Schlagel, and C. B. Dover, Phys. Rev. C **47** (1993) 1356
[18] T. A. Armstrong *et al.*, Phys. Rev. C **59** (1999) 2699
[19] T. A. Armstrong *et al.*, Nucl. Inst. Meth. A **437** (1999) 222
[20] P. Haridas *et al.*, Nucl. Inst. Meth. A **385** (1997) 412
[21] J. C. Hill *et al.*, Nucl. Inst. Meth. A **421** (1999) 431
[22] T. A. Armstrong *et al.*, Nucl. Inst. Meth. A **406** (1998) 227
[23] T. A. Armstrong *et al.*, submitted to Phys. Rev. C; N. K. George *et al.*, 15th Winter Workshop on Nuclear Dynamics, Park City, UT, January 13, 1999 (edt. W. Bauer *et al.*, Kluwer Academic/Plenum Publishers)
[24] S. Kabana, Nucl. Phys. A **638** (1998) 411c
[25] Private communication with I. G. Bearden for the NA44 Collaboration

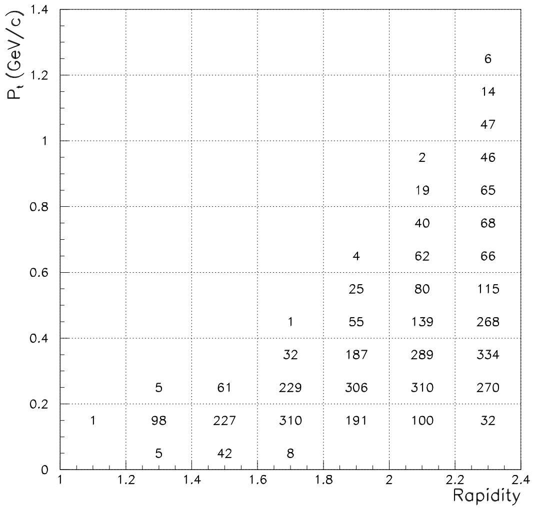

FIG. 1. Fractional geometric acceptance for antideuterons ($\times$1000) at the -0.75T field setting for E864 ($y_{cm} = 1.6$).

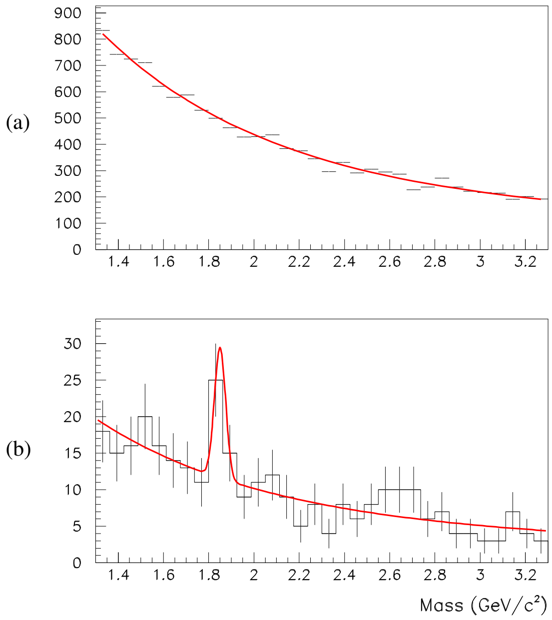

FIG. 2. Mass spectrum of charge $Z = -1$ particles ($1.8 < y < 2.2$) before (a) and after (b) a cut is placed on the energy deposited in the calorimeter to reduce background.

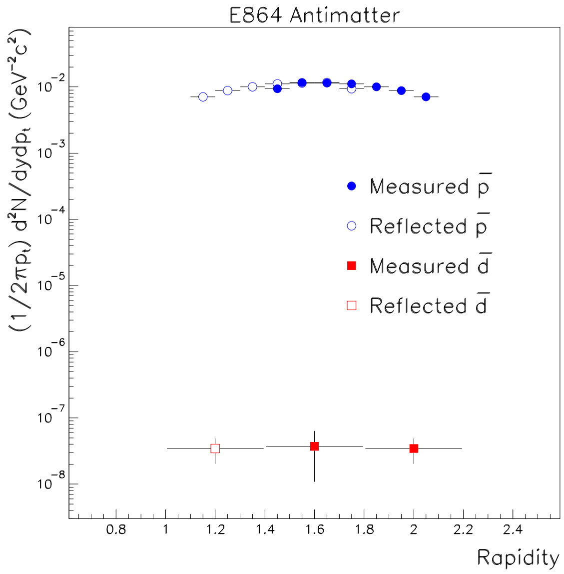

FIG. 3. Antimatter invariant yields measured by E864 in 10% central heavy ion collisions (statistical errors only).

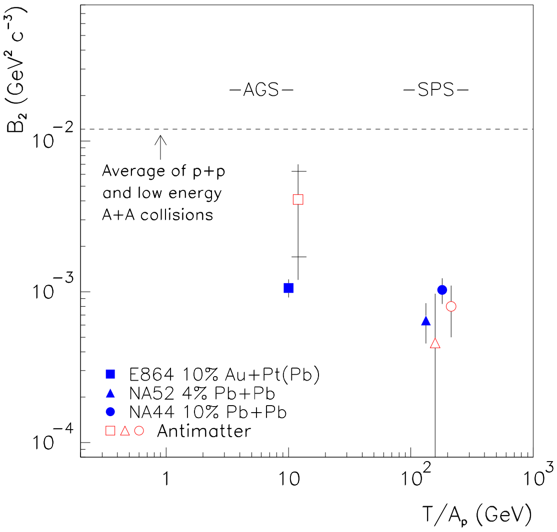

FIG. 4. Coalescence parameters for deuterons and antideuterons at the AGS and SPS [23–25]. Systematic errors of the E864 $\overline{B_2}$ measurement are shown as horizontal bars.